Journal Pre-proofs

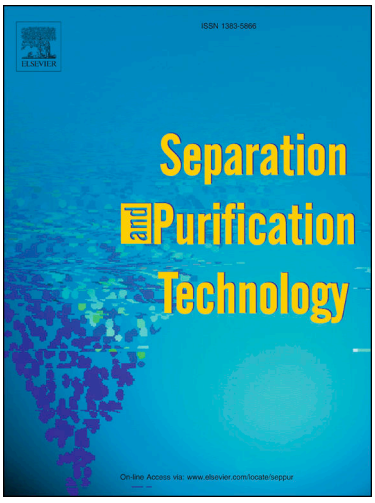

Performance of pressure stimuli-responsive nanofiltration and cellulose acetate forward osmosis membranes for PFOA contaminated wastewater treatment

Yahia Aedan, Ali Altaee, Ho Kyong Shon

PII: S1383-5866(25)01055-X
DOI: https://doi.org/10.1016/j.seppur.2025.132458
Reference: SEPPUR 132458

To appear in: *Separation and Purification Technology*

Received Date: 21 November 2024
Revised Date: 20 February 2025
Accepted Date: 9 March 2025

Please cite this article as: Y. Aedan, A. Altaee, H.K. Shon, Performance of pressure stimuli-responsive nanofiltration and cellulose acetate forward osmosis membranes for PFOA contaminated wastewater treatment, *Separation and Purification Technology* (2025), doi: https://doi.org/10.1016/j.seppur.2025.132458

Performance of pressure Stimuli-responsive nanofiltration and cellulose acetate forward osmosis membranes for PFOA contaminated wastewater treatment.

Yahia Aedan[1], Ali Altaee[1*], Ho Kyong Shon[1]

1: Centre for Green Technology, School of Civil and Environmental Engineering, the University of Technology Sydney, 15 Broadway, NSW, 2007, Australia

*Corresponding author email address: ali.altaee@uts.edu.au, tel: +0295149668

Authors statement

Yahia Aedan: Investigation, conceptualization, Data Analysis and curation, Validation, Writing – original draft, Writing – review and editing. **Ali Altaee:** Supervision, Methodology, Resources, Supervision, Conceptualization, Funding, Investigation, Data Analysis and curation, Writing – review, and editing. **Hokyong Shon:** Supervision, Data curation, Methodology, Writing – review and editing.

Declaration of interests

☒ The authors declare that they have no known competing financial interests or personal relationships that could have appeared to influence the work reported in this paper.

☐The authors declare the following financial interests/personal relationships which may be considered as potential competing interests:

Abstract

The persistent contaminant of Perfluorooctanoic acid (PFOA) in water bodies has been detected globally, which poses significant environmental and health risks. (add the technological limitation and difficulty to remove it) For the first time, pressure stimuli-responsive (PSR) technology utilized a nanofiltration (NF) membrane of specific characteristics operating as a forward osmosis (FO) process for PFOA treatment and compared their performance to a commercial FO cellulose triacetate (CTA) membrane. At 4 bar feed pressure, the pressure stimuli-responsive nanofiltration membrane (PSRNF) achieved 99.1% PFOA removal from wastewater compared to the 96.1% removal for the CTA membrane. Despite a lower average permeation flux of the PSRNF membrane at 0 bar applied pressure on the feed side, it maintained significantly higher flux rates at 2 bar, achieving 15.4 L/m²h, while the CTA membrane only achieved 6.4 L/m²h. At an applied pressure of 4 bar, the PSRNF membrane attained a flux of 39.53 L/m²h average permeation flux, six times greater than the CTA membrane. Fouling resilience advantage of the PSRNF membrane and high flux recovery when cleaned with DI water at 40°C, compared to the CTA membrane that required osmotic backwashing to achieve comparable results. The PSRNF membrane required only 0.011 kWh/m³ and 6 hours at 4 bar to achieve a 90% water recovery rate, which is > 86% less energy consumption than the CTA membrane that required 0.083 kWh/m³ and 41 hours to achieve the same recovery rate. The PSRNF TS80 membrane offers many advantages over the commercial CTA FO membrane, including one-tenth cost of FO membranes, more energy efficiency, and better fouling resistance, promoting the PSRNF membrane as an efficient option for PFOA-contaminated water treatment.

Keywords: Pressure stimuli-responsive membrane, PFOA, Forward osmosis, Wastewater, Filtration

1. Introduction

The widespread presence of perfluoroalkyl and polyfluoroalkyl substances (PFASs) in surface and groundwater has emerged as a significant contemporary issue. PFASs have attracted considerable global attention due to their persistence and toxicity in the environment, their potential for bioaccumulation, and the associated adverse health effects [1]. PFAS typically exhibit an aliphatic carbon structure, wherein hydrogen atoms are substituted entirely by fluorine or partially by fluorine [2]. They are recognised as highly fluorinated surfactants extensively used in various industrial sectors and consumer products such as food packaging, firefighting foams, apparel, protective coatings for textiles and carpets, electronics, and the production of fluoropolymers [3]. Among the PFASs prevalent in the environment, perfluorooctanoic acid (PFOA), chemically known as $C_7F_{15}COOH$, is extensively manufactured and frequently detected [4].

Full-scale water treatment system studies have demonstrated that conventional methods such as sedimentation, flocculation, coagulation, and filtration achieve less than 20% PFAS removal from water [7, 8]. Technologies utilising pressure-driven membranes, such as nanofiltration (NF), and reverse osmosis (RO), show promising results, achieving a high rejection rate (> 90%) of PFAS from contaminated wastewater [9]. The effectiveness of pressure-driven membrane separation relies on both membrane properties and filtration rate. Due to its denser

active layer, the RO membrane typically rejects more than 99% of PFAS, higher than the NF membranes but the latter membrane is more permeable and energy efficient [10]. An investigative study on the effectiveness of four commercially available RO membranes for treating wastewater from photolithographic processes with various concentrations of PFOS demonstrated over 99% rejection efficiency [11]. However, increasing PFOS concentrations were associated with flux decline. Furthermore, semiconductor wastewater containing isopropyl alcohol revealed a significant flux decline [12]. Another study investigated five commercial NF membranes (DK, NF90, XN45, NF270) to treat synthetic wastewater contaminated with PFAS. The rejection efficiency of these membranes varies from 66.0% to 99.9%, with DK and NF90 membranes exhibiting the highest rejections [13]. Also, the rejection rate of long-chain PFOA and PFOS was between 93% and 99.6%, higher than the short-chain PFAS compounds. The results highlight the significance of NF membrane structure in PFAS rejection, with tight-structure ones offering better rejection.

Moreover, variations in water properties, such as salinity and organic contents, can affect the membrane surface characteristics (surface charge and hydrophobicity) and subsequently affect PFAS rejection. PFAS rejection is also affected by feed pH, where the rejection efficiency is observed to be higher at alkaline pH levels, resulting from the increase of electrostatic repulsion occurrences among the negatively charged PFAS compounds and the surface of the membrane [14]. A study showed rising pH from 3.2 to 9.5 enhanced the surface charge of the NF membrane and increased PFOS rejection from 91.17% to 97.49% [15]. NF membrane rejection of PFAS is also affected by the feed composition. Research suggested that the presence of divalent ions such as Ca^{2+} and Mg^{2+} in the feed can increase the rejection efficiency [15, 16].

Despite the superior performance of RO and NF membranes in removing PFAS from wastewater, they are energy-intensive and susceptible to severe fouling. Alternatively, forward Osmosis (FO) membrane technology relies on natural osmotic processes without relying on external hydraulic pressure. In the FO membrane, freshwater moves from the lower osmotic pressure side to the side of higher osmotic pressure due to the osmotic pressure gradient; hence, there is no need for a high-pressure pump. This technology has been implemented in many applications due to its energy efficiency and lower fouling propensity compared to conventional wastewater treatment techniques [17]. Therefore, an innovative membrane development or modification is crucial to advance the advantages of the FO process, making it more efficient and cost-effective for wastewater treatment. A study by Yan et al. (2024) developed a novel PAN/CNTs/UiO-66-NH2 modified FO membrane that successfully removed heavy metals like antimony (Sb) and phenolic pollutants from wastewater [18]. An investigative study on FO membranes showed that the CTA FO membrane can achieve up to 99% removal efficiency of PFOA from wastewater without suffering permanent fouling, and its energy efficiency exceeds that of RO and NF membranes [19], as well as low operating costs. Despite these advancements, FO membranes have a limited water flux and are accompanied by the concentration polarization phenomenon (CP) and are affected by the dilution of the draw solution (DS), which decreases the osmotic gradient and subsequently reduces water flux. To enhance the permeation flux and subsequently increase water recovery of the FO membrane and to minimise CP, Pressure Assisted Forward Osmosis (PAFO) has been developed and investigated for wastewater treatments [20] and seawater desalination [21]. This concept is achieved by applying low pressure on the feed solution side to assist the osmotic pressure created by the draw solution side, subsequently increasing permeation flux and reducing CP [22]. An experimental study of PAFO in a hybrid desalination plant demonstrated achieving a water flux of 16.7 L/m^2h with 4 bar feed pressure and seawater brine draw solution with a concentration of 80 g/L [21]. Apart from the limited water permeability, FO membranes

are expensive when compared to state-of-the-art NF and RO membranes. Recently, a new filtration concept was tested, and outstanding water flux was demonstrated using pressure stimuli-responsive (PSR) NF membranes operating in the FO operating process [23].

The PSR concept uses high permeability and selectivity NF membranes that have a relatively high rejection rate to monovalent ions to reduce reverse salt flux. The PSRNF membrane must operate at low pressures on the feed side to stimulate water flux toward the draw solution side. Unlike FO membranes, water flux in the PSRNF membrane is negligible when there is no pressure on the feed side due to the membrane resistance. However, water flux in the PSRNF membrane increases exponentially with the feed pressure that should be applied to the active membrane layer to avoid its delamination. The ideal PSRNF membrane should have a small structure parameter (S) to reduce the CP phenomenon in the FO operation process, excellent selectivity to retain the draw solution without compromising the water flux, and be inexpensive [23]. The PSRNF membrane was applied for divalent ions removal from the seawater to reduce scale fouling in the thermal desalination plant [23]. Experiments with PSRNF TS80 (Microdyn®, USA) demonstrated a 1.4 times increase in water flux compared to CTA and TFC FO membranes under 4 bar feed-side pressure. Notably, the cost of the PSRNF TS80 is 10 times cheaper than the commercial FO membrane [23]. Despite the outstanding success of PSRNF membranes in seawater treatment, the concept has not been tested for the treatment of contaminated waters with forever contaminants, such as PFAS.

This study introduces the PSRNF technology, which utilizes a commercial NF TS80 membrane for PFOA-contaminated wastewater treatment. As the NF membranes are engineered to function with hydraulic pressure, the FO operation process was conducted with the feed solution against the selective membrane layer to prevent its delamination from the selective layer [24]. The investigation research questions are: i) What is the TS80 membrane performance in treating natural PFOA-contaminated wastewater? ii) Will TS80 fouling be reversible after chemical/physical cleaning? iii) What is the energy consumption for the treatment of PFOA-contaminated wastewater by the TS80 membrane? The selected PSRNF TS80 was compared with a CTA membrane under different transmembrane pressures (0, 2, and 4 bar) and different PFOA concentrations (5, 15, and 25 mg/L) in the TDS (FS) to evaluate PFOA rejection efficiency and to study the effect of feed solution (FS) concentrations on permeate flux. Furthermore, real wastewater was employed as the feed solution to achieve recovery rates of 75% and 90%, comparing the power consumption of our approach to other membranes and evaluating fouling mitigation.

2. Materials and Methods

2.1 Chemical reagents, wastewater, seawater, and membranes

All chemical reagents: Sodium Chloride (NaCl, 99% purity), Magnesium sulphate ($MgSO_4$, >99.5% purity), hydrochloric acid (HCl, 37% purity), sodium hydroxide (NaOH, 99% purity), and Perfluorooctanoic Acid (PFOA, 95% purity), were procured from Sigma-Aldrich (Australia). Wastewater contaminated with PFOA was sourced from electrokinetic soil remediation conducted in NSW, Australia.. Wastewater samples were stored in a refrigerator at three ^{o}C before use. The draw solutions (DS) were NaCl solution of 0.6M concentration and seawater obtained from Sydney (Australia). Synthetic and real wastewater from soil remediation were the feed solutions (FS) in the FO process. For the synthetic FS, three different PFOA concentrations of 5, 15, and 25 mg/L spiked in deionized (DI) water with neutralized pH. A commercially available flat sheet Cellulose Triacetate FO membrane (CTA) FTSH_2O™

was acquired from Sterlitech Corporation (USA), and a flat sheet thin-film Polyamide TS80 membrane from TRISEP® for the FO tests.

2.2 Characteristics of Membranes, seawater, and Wastewater

CTA membrane was selected due to its wide applications in FO studies and its high rejection rate of NaCl [25]. This asymmetric membrane has a dense active layer with an approximate contact angle of 68.2° ± 1° that produced moderate hydrophilicity [26], tolerance to up to 5 bar of hydraulic pressure and 50 ^{o}C feed temperature [27], and a structure parameter (S) of 707 µm [21] (Table 1). The latter is a function of the membrane thickness, tortuosity, and porosity. CTA natural hydrophilicity produces adequate membrane wetting, reducing the internal concentration polarisation (ICP) and increasing water permeability [28]. The commercial TS80 is a thin-film polyamide membrane in a flat-sheet configuration utilised as a softening membrane in many water purification applications, tolerant to damage from oxidants, and can handle a pH range between 2 and 12. The TS80 NF membrane has been selected due to the physicochemical characteristics that make it suitable for application in the FO process [23, 29]. The membrane has excellent water permeability (A_w) and salt permeability (B) that help retain the reverse diffusion of the draw solution to the feed solution. The water contact angle of the active membrane layer for the TS80 membrane (17.4^{o}±2.3) makes it more hydrophilic than the CTA membrane (68.1^{o}± 1), facilitating water permeation. Also, the membrane has a small structure parameter (S) to reduce internal concentration polarization (ICP). These characteristics are crucial in selecting the FO membrane. FO experiments were processed with the active layer (AL) facing the FS to prevent AL delamination under applied feed solution pressure [24]. Both membranes' water permeability (A_w) and salt permeability coefficients (B) were measured in a reverse osmosis test for one hour under 1 to 6 bar applied pressure and 25 ^{o}C. DI water was the FS to calculate the water permeability coefficient A_w (L/m^{2}h bar) for both membranes and water flux was calculated as the average value at various applied pressures (Equation 3). Two FSs of NaCl and $MgSO_4$ of 2 g/L concentration were used to calculate the salt permeability coefficient B (L/m^{2}h) according to (Equation 5).

Membrane surfaces were analysed by investigating the surface functional groups of the membrane samples before and the conclusion of the experiments by a Thermo Scientific Nicolet 6700 FT-IR spectrometer to conduct Fourier transform infrared (FT-IR) spectroscopy. The membrane samples for FTIR measurement were dried before characterisation and had at least 3 points scanned for repetition of spectra.

For the analysis of membrane surface structure and morphology, we employed advanced equipment to ensure the accuracy of our results. Scanning Electron Microscopy (SEM) using the EVO LS15 SEM instrument from Zeiss, Australia, was employed to analyse the new, fouled, and washed membranes. A sputtering machine (Leica EM ACE600) was employed to coat all samples with a thin layer (5 nm) of iridium (Ir) ~~of gold (5 nm)~~ at a current of 30 mA prior to SEM analysis to avoid the charge effects of the nonconductive samples. Energy dispersive X-ray (EDX) analysis was performed by using the Bruker SDD XFlash 5030 detector instrument (Zeiss, Australia. EDX analysis reveals the elemental composition of foulants, allowing for targeted cleaning strategies that enhance membrane performance and longevity.

For the analysis of wastewater and seawater, we employed highly precise inductively coupled plasma mass spectrometry (ICP-MS). The finding of this analysis is presented in (Table 2).

Malvern instruments measured the Zeta potential for the PSRNF TS80 and FTSH_2O CTA FO membranes. Wettability and hydrophilic properties were assessed by measuring the contact angle at different points on the same membrane. The sessile drop method was employed for these measurements, by FACE Automatic Interfacial Tensiometer from Japan.

Table 1. Characteristics of PSRNF TS80 and FTSH_2O CTA membranes.

Membrane	**A_w (L/m²h.bar)**	**B (L/m²h)**	**S (µm)**	**NaCl Rj (%)**	**$MgSO_4$ Rj (%)**	**Zeta potential (mV)**	**Contact angle**
TS80	13.1	2.38*** 0.69****	310	84	98.66	-55.6	17.4°±2.3*
FTSH_2O (CTA)	0.73	0.52*** 0.209****	707	89	97.84	-12.8 ± 1.2	68.1°± 1* 60.2°± 0.5**

*contact angle of the active layer. **contact angle of the support layer. ***B for NaCl. ****B for $MgSO_4$.

Table 2. Characterization and analysis of wastewater samples

Parameter	**Measurement instrument**	**Wastewater**	**Seawater**
Conductivity	LAQUA meter (Horriba, Japan)	1.871 ±3 ms/cm	54.8 ± 1 ms/cm
PFOA	LC-MS (SHIMADZU, Japan	17.92 ±3 mg/L	-
Total dissolved Solids	LAQUA meter (Horriba, Japan)	1752 ± 0.5 mg/L	27500 ± 100 mg/L
pH	LAQUA-pH meter (Horriba, Japan)	9.7	7.3

Mn	ICP-MS (Agilent, United States)	1710 ± 20 mg/L	85 ± 0.5 mg/L
Si	ICP-MS (Agilent, United States)	10 ± 0.5 mg/L	-
K	ICP-MS (Agilent, United States)	14.9 ± 0.1 mg/L	338 ± 1 mg/L
Mg	ICP-MS (Agilent, United States)	1.12 ± 0.1 mg/L	1151.5 ± 4 mg/L
Cl	ICP-MS (Agilent, United States)	33.5 ± 2 mg/L	1858.5 ± 3 mg/L
Ca	ICP-MS (Agilent, United States)	0.9 ± 0.1 mg/L	400 ± 5 mg/L
Na	ICP-MS (Agilent, United States)	27.3 ± 3 mg/L	1385 ± 3 mg/L

2.3 System setup

A Sterlitech cast acrylic clear cell CFO42A-FO was used, with the CTA and TS80 membranes placed inside. The exterior dimensions of the cell are 4 x 5 x 3.25 inches, accommodating an actual membrane used area of 42 cm^2. The acrylic cell has a 17 mL holding volume on either side of the membrane and features two cross channels on both sides. The cell can tolerate a maximum hydraulic pressure of 27.6 bar and a temperature of 88 ^oC. Two F-550 flow meters (Blue-White et al., DC, USA) were connected to the cell, one on each side, along with a pressure gauge (USG US Gauge) reading up to 6 bars connected to the feed solution side for hydraulic pressure measurements. Two gear pumps (Cole-Parmer) were incorporated into the setup to maintain a steady flow for FS and DS at two Liters per minute (LPM) in the setup **(Figure 1)** to maintain solutions circulation on both sides. The setup was connected to two beakers, one for the DS and one for the FS sides. The beaker on the FS side was placed on a digital scale balance (A&D EK-15KL) connected to a computerized system for permeation variation recording travelling to the DS beaker side through the membrane. A portable conductivity and Total Dissolved Solids (TDS) meter (HQ 14d, HACH, Australia) was used to measure the TDS and salinity of both solutions (before, throughout, and at the end of each experiment). At the beginning and end of each experiment, samples from the FS and DS were collected and stored in a cool room at a temperature of 3 ^oC for further analysis.

2.4 PFOA detection

PFOA concentrations in both the feed and permeate were measured (at the start and conclusion of each experiment) using ultra-performance liquid chromatography-mass spectrometry from (SHIMADZU in Japan). A column (KINETEX LC18) with measurements of 100×2.1 mm was

used and coupled with a mobile phase consisting of ammonium acetate and acetonitrile (30/70, v/v), with a flow rate of 0.2 mL/min and 10 µL sample injection volume. The analytes, with a specific mass-to-charge ratio (m/z) of 499.05, were measured using selected-ion monitoring (SIM). ASTM 7979-17 Protocol was followed for sample dilution [30]. The calibration for PFOA was conducted using a five-point standard curve, with concentration levels ranging from 0.1 to 20 µg/L. Linear regression with inverse concentration weighting was used to fit the calibration curves, and each analytical run achieved an R^2 value greater than 0.995. After concluding each experiment, the membrane was removed from the FO cell and soaked in (LC-grade) methanol for 10 hours in a thermostatic shaker at room temperature to desorb any attached PFOA from the membrane coupon. The desorbed PFOA concentration in the solution was measured similarly to the feed and permeation solution, and the rejection efficiency of the membranes was adjusted by considering the desorbing PFOA. Control experiments were conducted without membranes to confirm that the FO cell and tubing would not absorb PFOA and affect the experimental outcomes. After running the experiments without membrane with DI water for 30 minutes, samples of DI water were tested. The results of the samples indicated that no PFOA was detected (or below the detection level). After each experiment, the system was cleaned using detergent, DI water, and a methanol rinse, and then it was allowed to dry in a fume hood for subsequent use.

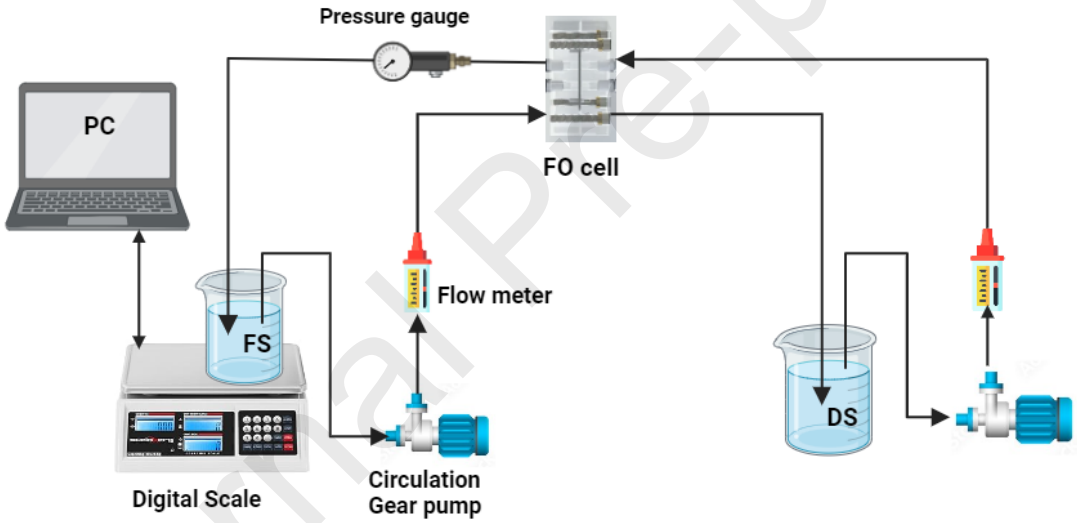

Figure 1. Forward osmosis filtration unit

2.5 Data Analysis

Permeation flux of the membranes, which describes the rate of water passing through the membrane from FS to DS, was calculated by computing the weight variation of the FS throughout the experiment in the following equation:

$$F_w = \frac{\Delta W}{A * \Delta t} \qquad \text{(Equation 1)}$$

Where Fw is the membrane permeation flux (L/m²h), ΔW represents the weight variation of the FS measured in (Kg), while A is the active area of the membrane in m², and Δt refers to the

time duration measured in hours (h). The reverse salt flux (Fs), which is the salt diffusion across the membrane in (g/m^{2}h), can be calculated as the following equation:

$$F_s = \frac{C_f m_f - C_i m_i}{At} \quad \text{(Equation 2)}$$

Where c_i (g/L) and m_i (L) represent the feed solution's initial concentration and volume, respectively, similarly, C_f (g/L) and m_f (L) are the solute concentration and the volume of the feed solution measured at the time t, respectively. The water permeability A_w (L/m^{2}h) was calculated by the following equation:

$$A_w = \frac{F_W}{\Delta P} \quad \text{(Equation 3)}$$

In Equation 3, ΔP (bar) is the applied pressure in the RO dead-end cell. Determination of the rejection efficiency of the membrane (R_E) as a percentage was calculated by utilising the following equation:

$$R_E = \left(1 - \frac{C_d}{C_f}\right) \times 100 \quad \text{(Equation 4)}$$

C_d and C_f represent the concentration of DS and FS in (g/L), respectively. Equation 5 was employed to determine the salt permeability coefficient (B) as a function of the membrane permeation flux and rejection rate.

$$B = \frac{(1 - R_E)}{R_E} * F_w \quad \text{(Equation 5)}$$

The flux reduction of the membrane (F_R) was determined following a 30-minute membrane washing process, which involved using hot DI water at 40°C or backwashing for 30 minutes with 0.6M NaCl on the AL and 40°C DI water on the selective layer (SL). This procedure was used to assess the efficiency of the physical washing method in restoring permeation flux and allowing the membrane to be reused for the same experimental protocols. Equation (6) was used to calculate the flux reduction:

$$F_R = \left(1 - \frac{F_a}{F_{wa}}\right) \times 100 \quad \text{(Equation 6)}$$

F_{wa} represents the pristine membrane's average water flux, and F_a is the average permeation flux for the cleaned membrane. The recovery rate is determined by calculating the ratio of the permeate flow to the feed flow, as expressed by the following equation:

$$Rc = \left(\frac{J_p}{J_f}\right) \times 100\% \quad \text{(Equation 7)}$$

In Equation (7), J_p and J_f represent the flow rate of the permeate and the FS (L/min), respectively.

The membrane-specific power consumption (Ps) in kWh/m^3 was calculated according to the following equation:

$$P_s = \frac{P_f Q_f + P_i Q_i}{\eta * Q_p} \quad \text{(Equation 8)}$$

In the prefiltration phase, the energy consumed by the prefiltration method (E), which may be incorporated into the prefiltration of wastewater process when relevant, was calculated using the following equation:

$$E = \frac{P_f Q_f}{\eta * Q_p} \quad \text{(Equation 9)}$$

P_f is the hydraulic pressure of the wastewater (bar), and P_i is the hydraulic pressure of the seawater (bar). Q_f and Q_i represent flow rates in m^3/h for the wastewater and seawater, respectively, while η represents the circulating pump efficiency (0.85 in this study), and Q_p represents the permeate flow rate in m^3/h.

The average radius of the pores for the membranes was calculated using the Guerout–Elford–Ferry equation to measure the average pore radius of the membrane (R_m).

$$R_m = \frac{\sqrt{(2{\cdot}90 - 1.75\mathrm{p})8hTF_W}}{\mathrm{p}PA} \quad \text{(Equation 10)}$$

Where h represents water viscosity (Pa s), F_W is the permeation flux per unit time, P is operational pressure (MPa), A is the membrane effective area, T is membrane thickness, and p is membrane porosity, which was calculated according to the following equation:

$$\mathrm{p} = \frac{(\omega_1 - \omega_2)/\rho_\omega}{(\omega_I - \omega_2)/\rho_w + \omega_2/\rho_\rho} \quad \text{(Equation 11)}$$

ω_1 and ω_2 are the weights of the wet and dry membranes in (g), ρ_ω is water density (1.00 g/cm^3), and ρ_ρ is the density of the polymer. Water flux decline (%) was calculated as the ratio of the water flux at any time (J_t) to the initial water flux (J_o) as follows:

$$Water\ flux\ decline = \left(1 - \frac{J_t}{J_o}\right) * 100 \quad \text{(Equation 12)}$$

3. Results and discussion

3.1 Permeation flux

A set of FO experiments was conducted to evaluate water flux in the PSRNF TS80 and the commercial FTSH2O CTA FO membranes. Each experiment ran for six hours in this set of experiments. The DS was 0.6M NaCl, and FS contained 5 mg/L PFOA spiked in deionized

(DI) water, with incremented applied hydraulic pressure on the FS of 0, 2, and 4 bar. In both PSRNF and CTA membranes, the feed pressure was applied to the FS to enhance permeation flux. In addition to improving permeation flux, the FS must be against the active membrane layer in the PSRNF to protect it from delamination. Feed pressures ranging from 0 to 4 bar were found sufficient to counteract the resistance of the PSRNF membrane [23]. Thus, and for comparison purposes, the PSRNF and CTA membrane tests were conducted under the same feed pressure and with the feed solution facing the active layer (ALFS).

The FO tests revealed that the initial permeate flux for the CTA membrane increased with increasing applied pressure due to driving force elevating, and 8.47, 16, and 24.57 L/m^{2}h water flux were recorded for 0, 2, and 4 bar applied pressures (Fig2A). Under the same FS side applied pressure, the initial water flux for the TS80 membrane was 7.71, 32.7, and 56.2 L/m^{2}h. The initial water flux for both membranes increased significantly with the applied hydraulic pressure, nearly doubling at 2 bar and tripling at 4 bar, specifically for the CTA membrane, while the PSRNF TS80 membrane responded much higher and increased exponentially to more than 4 times with 2 bar and further to almost eight times at 4 bar hydraulic pressure, due to its higher hydrophilicity and water permeability coefficient which is 18 times more than the CTA membrane (Table 1). However, the permeate flux for the CTA membrane decreased by almost 40% to 9.55 L/m^{2}h and 44% to 13.67 L/m^{2}h after one hour of operation at 2 and 4 bar, respectively. It then continued to decline steadily, recording 7.84 and 9.71 L/m^{2}h at the conclusion of the experiments due to the dilution of the DS.

The water flux in the PSRNF membrane was minimal during the FO operating process at 0 bar due to the membrane resistance to water flux, but it exhibited an exponential elevation in the water flux with the hydraulic pressure increase. At the end of the tests, the permeate flux decreased by 31% to 22.41 L/m^{2}h at 2 bar and 21.6% to 44.07 L/m^{2}h at 4 bar during the first hour due to the substantial initial flux diluting the DS, which in turn reduced the osmotic pressure (Fig 2A). Despite the PSRNF membrane's higher water flux leading to faster dilution of the draw solution (DS) compared to the CTA membrane, the reduction in water flux by the end of the PSRNF membrane tests was less significant than that observed in the CTA membrane (Fig 2A). The results indicate that permeation flux in the PSR membrane is strongly responsive to the applied feed pressure due to its high water permeability.

The average water flux for the CTA membrane at 0 bar was 7.65 L/m^{2}h, achieving an 18% recovery rate. With 2 bar pressure, the average permeate flux increased by 13% to 8.65 L/m^{2}h, and with 4 bar pressure, it further increased by 54% to 11.82 L/m^2·h. The recovery rates were 18.9% and 24.5% for the CTA membrane at 2 and 4 bar. The PSR TS80 membrane had a lower average permeate flux of 5.9 L/m^{2}h and a 13.5% recovery rate at 0 bar hydraulic pressure due to higher membrane resistance. Conversely, the TS80 membrane's average permeate flux at 2 and 4 bar increased by nearly 3.6 and 7.2 times to 21.13 L/m^{2}h and 42.87 L/m^{2}h, with recovery rates of 48.6% and 98%, respectively. The thick structure parameter of the CTA membrane resulted in an intensive CP, significantly reducing water flux compared to the TS80 membrane, which has an 80% thinner support layer (Table 1). The results also show that the CTA membrane is less responsive to increasing applied pressure, achieving a 54% average water flux increase as feed pressure increased from zero to 4 bar, while the PSRNF membrane achieved >600% average water flux increase (Figure 2B). Besides, the CTA membrane is more affected by CP and dilution of the DS, resulting in reduced osmotic pressure. Although the TS80 membrane initially displayed a lower average permeate flux without applied hydraulic pressure compared to the CTA membrane, it demonstrated greater responsiveness to low hydraulic pressure and experienced less CP, making the TS80 membrane a better choice for

achieving a higher average permeation flux under low hydraulic pressure **(Figure 2B)**. The membrane selectivity (*Fs/Fw*) was measured and compared for both membranes at 0, 2, and 4 bar feed pressures. Results indicated that at 0 bar, the CTA membrane has a slightly better selectivity compared to the PSRNF membrane **(Figure 2C)**. In contrast, at 2 and 4 bar applied pressure, the PSNRF membrane selectivity outperformed the CTA membrane by 76% and 84%, respectively **(Figure 2C)**. The reason for this is the greater water flux in the PSRNF membrane, which is a function of the applied feed pressure, while membrane rejection is maintained since it is a function of the membrane's intrinsic characteristics.

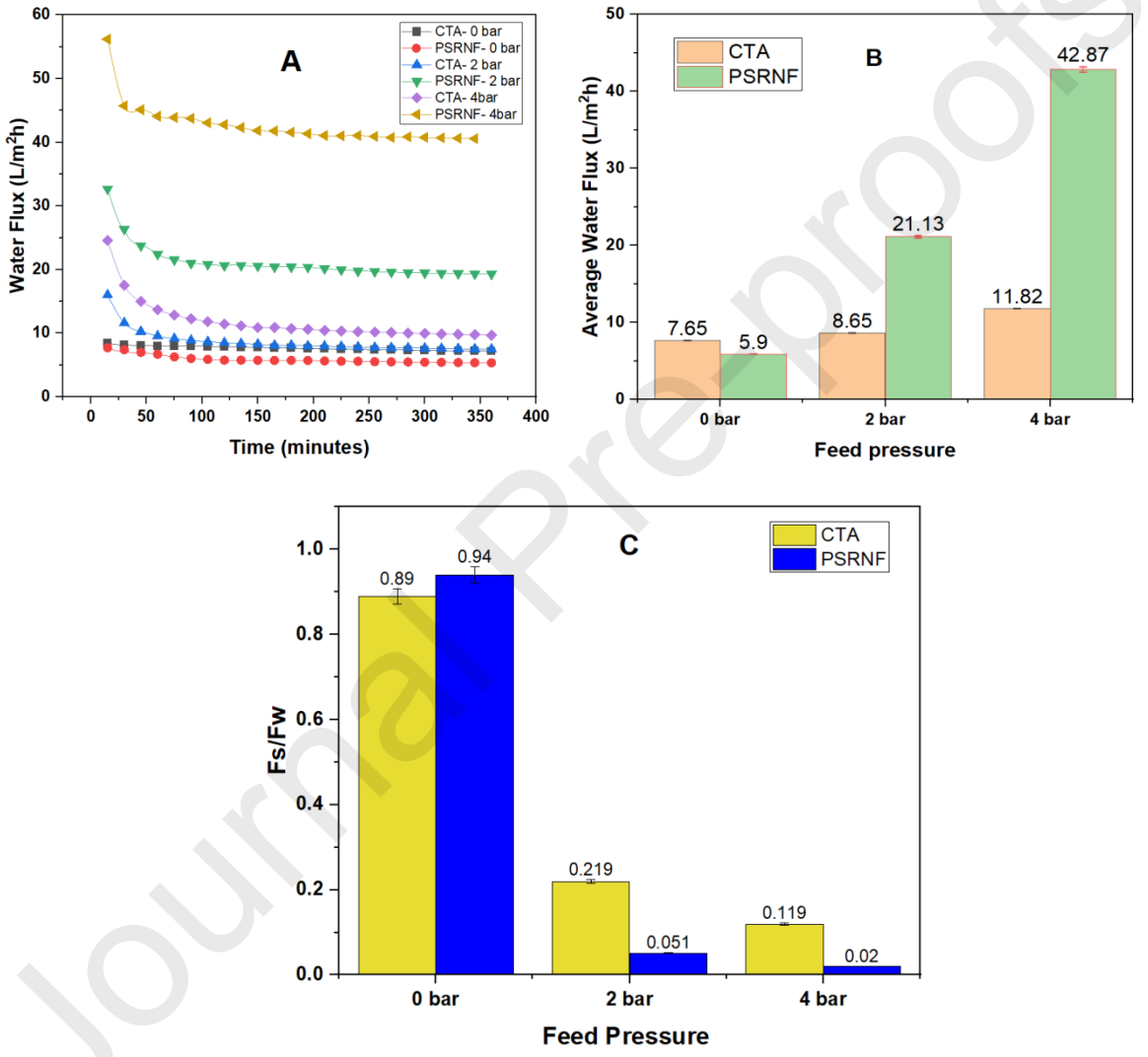

Figure 2. A) Water flux for the CTA and PSRNF membranes with the three different SR-feed pressure (0, 2, and 4 bar), B) Average water flux for CTA and PSRNF membranes with different SR-feed pressure, C) Membrane selectivity for CTA and PSRNF membranes with different SR-feed pressure.

3.2 Impact of PFOA Concentration on Rejection

To investigate the impact of contaminant concentrations on the membrane rejection efficiency, three PFOA concentrations (5, 15, and 25 mg/L) spiked in DI water and tested with both CTA and PSRNF membranes, applying 0, 2, and 4 bar pressures on the FS side while the DS was 0.6M NaCl. The PFOA rejection efficiency for the CTA membrane was 98% at 0 bar across all PFOA concentrations in the FS (Fig.3A). In contrast, the PSRNF membrane had a slightly lower rejection efficiency compared to the CTA membrane, achieving 97% for the same FS concentrations (Fig.3A). Interestingly, the increases in FS concentrations did not affect both membrane's average permeation fluxes. The greater rejection of the CTA membrane is related to its lower salt permeability coefficient (B) compared to the PSRNF TS80 membrane (**Table 1**). Also, the higher water flux in the CTA at 0 bar led to a greater dilution of the draw solution (Equation 4) and hence increased the membrane rejection. Applying 2 bar pressure, the rejection efficiency for the CTA membrane showed a slight increase by 0.2% and 0.5% compared to the 0 bar applied pressure for the 5 and 15 mg/L FS concentrations, and further by 0.9% for the 25 mg/L concentration, achieving 98.2%, 98.5% and 98.90% rejection efficiency (Fig. 3B). There was no noticeable change in the average permeate flux as the concentration of PFOA increased from 5 mg/L to 15 mg/L. However, a 3.30% decrease in average permeation flux was observed when the FS concentrations increased to 25 mg/L, recording 8.37 L/m²h. The slight increases in rejection efficiency and decrease in permeate flux with rising PFOA concentrations in FS are likely due to the compression effect, which might clog the membrane's pores and elevate CP. The mechanisms of PFOA retention by CTA FO membranes include size exclusion and electrostatic repulsion between the negatively charged membrane and PFOA molecules. Hydraulic pressure on the FS side promotes PFOA accumulation and adsorption on membrane surfaces or within pores, increasing membrane resistance, fouling, and pore-clogging, thereby reducing permeate flux. Furthermore, as water molecules selectively permeate the membrane, the concentration of PFOA at the surface of the membrane increases relative to the bulk feed stream. This phenomenon is particularly pronounced under hydraulic pressure, which increases the surface concentration and leads to concentration polarization (CP) and reduced permeation flow. As a result, the higher PFOA concentration at the membrane surface enhances PFOA rejection due to more pronounced steric effects. As PFOA accumulates on the surface of the membrane continuously, its concentration on the membrane surface can eventually exceed the critical micelle concentration [14], leading to the formation of PFOA micelles on the membrane, increasing the molecular size and improving the separation efficiency [31]. Under 2 bar applied pressure on the feed side, the average water flux for the PSRNF membrane showed no significant differences as the feed solution (FS) concentration increased from 5 mg/L to 15 mg/L and 25 mg/L, recording approximately 21.94 L/m²h. Nevertheless, the rejection efficiency increased to 97.3%, 97.6%, and 98.1% for the three PFOA concentrations (Fig.3B). These elevations in rejection efficiency stemmed from increasing permeation flux, increasing PFOA concentration in the FS and enhancing the membrane rejection efficiency [15, 16]. The accumulation of PFOA near the membrane surface typically increases with the increase of PFOA concentration in the FS, which subsequently changes the surface characteristics of the membrane, leading to a higher charge repulsion and, consequently, leading to a higher PFOA rejection. As the applied pressure in the CTA membrane increased to 4 bar, the rejection efficiency for PFOA concentration of 5 mg/L was almost similar to the 2 bar applied pressure of 98.2%, despite the higher average water flux of 11.82 L/m²h. For the 15 and 25 mg/L concentrations, PFOA rejection reduced to 98.1 % and 98 %, respectively (Fig.3C). This might be because differential pressure plays a more dominant role in separation as pressure increases, reducing the effectiveness of the size exclusion, electrostatic repulsion, and adsorption in retaining PFOA, resulting in a lower PFOA removal rate [32]. There was also a reduction in average permeation flux by 1.8% and 9.1%, compared to the 5 mg/L feed concentration, recording 11.61 L/m²h

and 10.75 L/m²h for the 15 mg/L and 25 mg/L of PFOA concentrations, respectively (Fig.3C). The PSRNF membrane rejection efficiency at 4 bar feed pressure increased to 99% for the three PFOA concentrations. This increase in the rejection efficiency is attributed to the higher water flux for the PSRNF membrane, which is doubled at the applied pressure of 4 bar compared to the 2 bar, diluting the PFOA concentration in the draw solution side. At 4 bar applied pressure, the average water flux for the PSRNF membrane decreased by 1.22% and 1.78% with the increase of PFOA concentrations to 15 mg/L and 25 mg/L, resulting in water fluxes of 42.36 L/m²h and 42.12 L/m²h, respectively (Fig.3C). As a pressure-driven membrane, the TS80 NF membrane exhibits considerable resistance to water flux when operating at zero feed pressure. However, the PSRNF membrane water flux increases exponentially with the feed pressure due to its high permeability compared to the conventional CTA membrane. In comparison to the CTA membrane, the PSRNF TS80 membrane offered comparable or even better rejection rates as applied pressure on the feed side increases from 0 to 4 bar and considerably higher water flux at all feed pressures, exhibiting outstanding performance when it is used in the FO process.

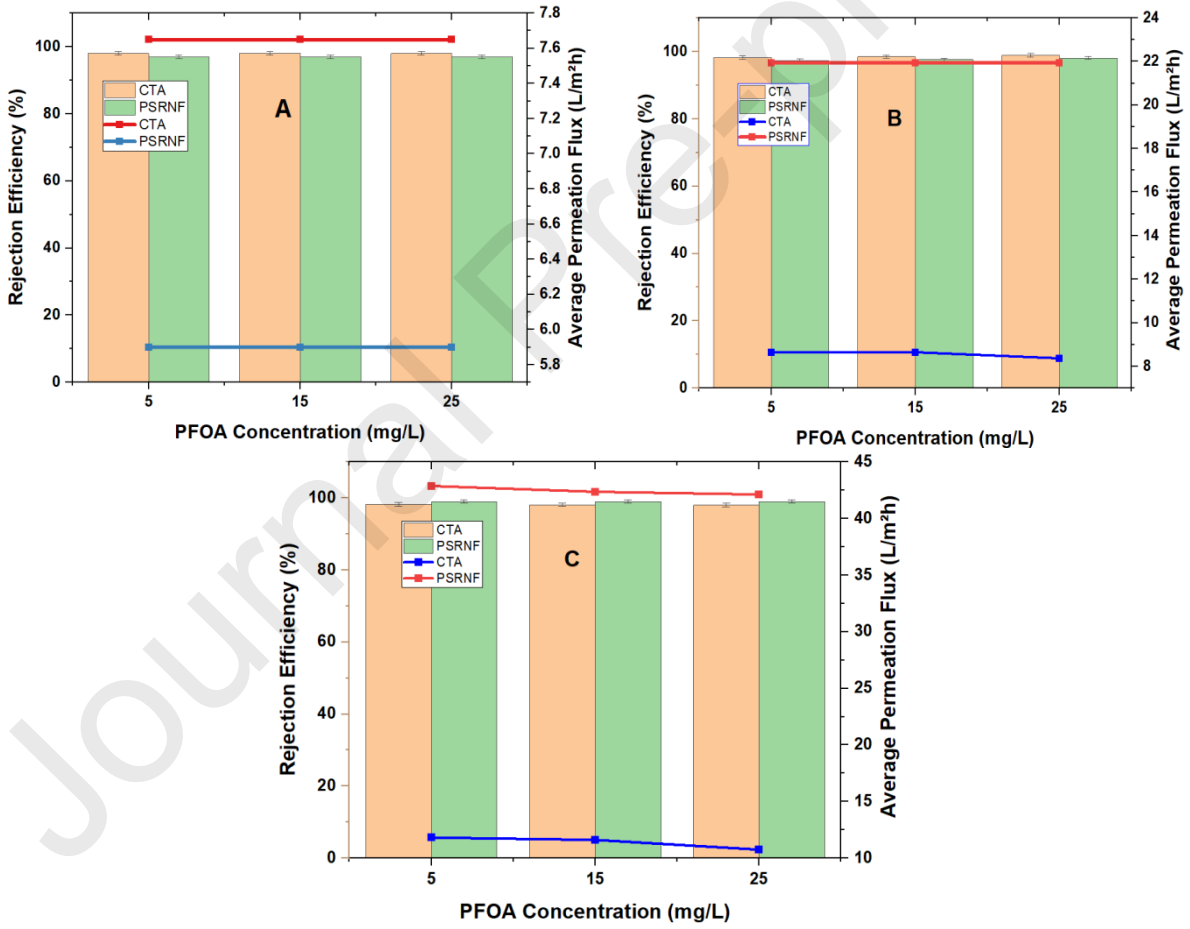

Figure 3. Rejection efficiency and average permeation flux for the CTA and PSRNF membranes with three different PFOA concentrations of (5, 15, and 25 mg/L) in the FS, A) 0 bar feed pressure, B) 2 bar feed pressure, and C) 4 bar feed pressure. The solid line represents the average permeation flux, and the column data represents the rejection efficiency.

3.3 Wastewater and fouling

This set of experiments evaluated the performance of the PSRNF TS80 membrane performance for actual PFOA-contaminated wastewater treatment. Wastewater sourced from the soil remediation process with 17.9 mg/L of PFOA at a pH of 9.7 was used as the FS, and seawater as the draw solution (**Table 2**). The PFOA wastewater was pre-filtered using a Durapore® Membrane Filter (0.45 μm, Sigma-Aldrich, Australia) before the experiments, and seawater pH of 7.3 served as the DS. All experiments with the PSRNF TS80 membrane were conducted at 2 and 4 bar since the water flux for the membrane was insignificant at 0 bar. All experiments continued until 90% recovery rates were achieved.

For fouling mitigation and membrane cleaning, the PSRNF membrane was cleaned with 40°C DI water and 3 LPM flow rate on both sides for thirty minutes after concluding the experiment. Cleaning protocol with 40 °C DI water showed an efficient way for dissolving and removing foulant materials from the membrane surface [33]. The initial permeate flux during the first cycle of the PSRNF membrane was 32.60 L/m²h, then it decreased by nearly half to 16.18 L/m²h after two hours of operation due to the dilution of the DS and probably the accumulation of foulant materials on the membrane's AL surface. The flux then gradually declined further, reaching 14.34 L/m²h by the experiment conclusion **(Figure 3A)**, with an average water flux of 15.40 L/m²h **(Figure 4B)**. The initial permeation flux in the second filtration cycle for the washed PSRNF membrane was 32.10 L/m²h, which declined after two hours to 16.03 L/m²h and then constantly declined, reaching 13.33 L/m²h after 16.25 hours. **(Figure 4A)**. The average water flux in the second filtration cycle was 14.85 L/m²h, or 3.57% less than the first cycle **(Figure 4B)**. Then, the PSRNF membrane was washed with DI water at 40 °C, resulting in an average water flux of 14.68 L/m²h during the third filtration cycle, reflecting a decline of 4.6% in water flux compared to the first cycle (**Figure 4B**). The membrane PFOA rejection efficiency was 98.5%. Compared to the results from section 4.1, where the feed pressure was 2 bar and 15 mg/L PFOA concentration, there was a slight increase in the rejection efficiency by 0.9%, probably resulting from the interaction between the monovalent and divalent ions (Na^+, Mn^{2+}, Mg^{2+}, and Ca^{2+}) in wastewater and the PFOA head functional groups. This interaction caused an apparent increase in the molecular weight (MW) of PFOA, thereby further enhancing its removal by the membrane [34]. Also, the alkaline wastewater of pH 9.7 resulted in more negative charge on the membrane surface, increasing electrical repulsion with the negatively charged PFOA molecules and membrane rejection. Cations and anions in the wastewater (Table 2) will increase the solution's ionic strength, a phenomenon that is likely to shrink the membrane pores. Previous studies have demonstrated that increasing the ionic strength of a solution can lead to a reduction in membrane pore size due to electrostatic compression. Higher concentrations of ions shield the charges on the membrane surface, which reduces electrostatic repulsion within the membrane matrix. This effect causes the polymer to contract, ultimately decreasing the effective pore size [35]. Therefore, increasing the solution ionic strength will also contribute to PFOA rejection by the PSRNF membrane.

At 2 bar feed pressure, the initial permeate flux for the CTA membrane was 16.76 L/m²h, dropped by almost half after the first hour, then gradually declined, reaching 5.62 L/m²h by the end of the experiment (**Figure 4A**). The CTA filtration process lasted 38.5 hours to achieve a 90% recovery rate, with an average permeation flux of 6.40 L/m²h. Similarly, cleaning the membrane with 40°C DI water and a flow rate of 3 LPM on both sides for thirty minutes. When the experiment was repeated, there was a significant 16 % decline in average permeation flux. It concludes that this washing method was not adequate to restore the membrane flux due to the deposition of foulant on the membrane surface. Fouling materials first settle on the

membrane through convective deposition and then chemically bind to the layer of accumulated material. Besides, the interaction between organic and inorganic components in wastewater accelerates the aggregation of these fouling materials. Increasing the membrane resistance and the long duration of the experiment resulted in further compaction of fouling materials on the membrane surface. An osmotic backwash was carried out for the CTA membrane cleaning using 0.6 M NaCl on the AL and DI water on the SL for 30 minutes, both at 40°C and without applying any pressure. Backwashing demonstrated positive cleaning outcomes in removing fouling from the membrane's surface and pores by pushing fouling materials out of the membrane pores when freshwater penetrates the membrane's pores [36]. It also eliminates secondary wastewater generation at the end of the cleaning process. This backwashing resulted in only a 3.6 % decline in average permeation flux, reducing it to 6.16 L/m²h compared to the average water flux in the first filtration cycle (**Figure 4D**). The membrane was washed again using the same backwashing protocol, and a third filtration cycle showed a less than 4.9 % average water flux decline, resulting in a flux of 6.08 L/m²h (**Figure 4B**). These results indicate that backwashing was effective in restoring the membrane permeation performance. The PFOA rejection efficiency for the CTA membrane was 96.1% which is almost 2.5% lower than section 4.1. Despite the presence of monovalent and divalent ions in the FS wastewater, which bind with PFOA and increase MW and, therefore, increase PFOA retention, there was a decrease in rejection efficiency. This may be due to the higher pH of the wastewater, which could cause pores swelling. As the FS's pH becomes more alkaline, the functional groups of the CTA membrane dissociate, which causes the negatively charged polymer chains to repel each other, thereby enlarging the membrane's pores. As the pores enlarge, more solute can pass through, which reduces the membrane's effectiveness at blocking PFOA [37]. Separate experiments were conducted at 2 bar feed pressure to investigate the impact of alkaline pH on membrane water flux by adjusting the wastewater pH to 7 for both the CTA and PSRNF TS80 membranes. Water flux in the CTA and PSRNF membranes was 6.4 L/m²h at pH 9.7 and 5.86 L/m²h at pH 7, recording 8.4% lower water flux at pH 7. The corresponding water flux for the PSRNF TS80 membrane was 15.4 L/m²h at pH 9.7 and 15.18 L/m²h at pH 7, showing an insignificant change in the water flux (1.4%) due to feed pH variation. Generally, the PSRNF TS80 membrane tolerates a wider range of feed pH, from pH 1 to pH 12, making it more resistant to pH change than the CTA membrane.

Additionally, the average radius of the pores for the CTA and PSRNF membranes was calculated for both alkaline and neutral wastewater using Equations 10 &11. Results indicated a 6.1% reduction in pore size for the CTA membrane in neutral wastewater compared to alkaline wastewater, while only a 1.2% reduction in pore radius was observed for the PSRNF membrane, confirming that the PSRNF TS80 membrane is more tolerant to higher alkalinity than the CTA membrane. At 4 bar applied pressure, the average permeation flux for the PSRNF membrane was 39.53 L/m²h. There was only a 2.9 % reduction in the average permeation flux to 38.40 L/m²h for the second cycle, followed by 4.5 % to 37.75 L/m²h for the third cycle after washing the membrane with DI water at 40 °C (**Figure 4D**). The PSRNF membrane PFOA rejection efficiency increased further to almost 99.1% resulting from the increasing of permeation flux compared to 2 bar pressure. At a 4 bar pressure and CTA membrane, the average permeation flux of the first filtration cycle was 6.54 L/m²h and lasted 41 hours to achieve the 90% recovery rate compared to 6 hours for the PSRNF membrane. Backwashing the membrane resulted in a 3.6% decline in the average permeation flux to 6.30 L/m²h for the second cycle and further declined by 5.1% to 6.20 L/m²h for the third cycle after undergoing backwashing again (**Figure 4D**). Furthermore, there was no noticeable change in the CTA membrane's rejection efficiency for PFOA when comparing 2 bar pressure to 4 bar pressure.

This lack of change could be related to increased pore clogging, which could lead to further retention of PFOA.

Generally, the PSRNF TS80 membrane demonstrated better water flux, competitive rejection rate, lower maintenance, and excellent fouling resistance than the CTA membrane. It is recommended to operate the PSRNF membrane at a moderately low pressure of 4 bar. Cleaning the PSRNF TS80 membrane with DI water at 40 ^{o}C was sufficient to restore over 95% of the water flux after three filtration cycles at a 90% recovery rate, while the CTA membrane required a more sophisticated osmotic backwash for cleaning. The PSRNF TS80 excellent rejection, 84% of NaCl and 98% of MgSO4, reduced the RSF, while its high water flux diluted the concentration of the draw solution in the boundary layer that is responsible for the salt diffusion from the draw to the feed side. The small structure parameter of the PSRNF TS80 membrane alleviated the impact of ICP. Finally, the impact of the concentrative CP was reduced due to operating the PSRNF membrane in the PRO mode, the active layer facing the feed solution. As a result, membrane fouling was fairly easy to mitigate by osmotic DI water at 40 ^{o}C. Moreover, the PSRNF membrane achieved 90% recovery after 6 hours when it operated at 4 bar compared to 41 hours for the CTA to achieve a 90% recovery rate, underlining the superiority of the PSRNF membrane in the FO process applications.

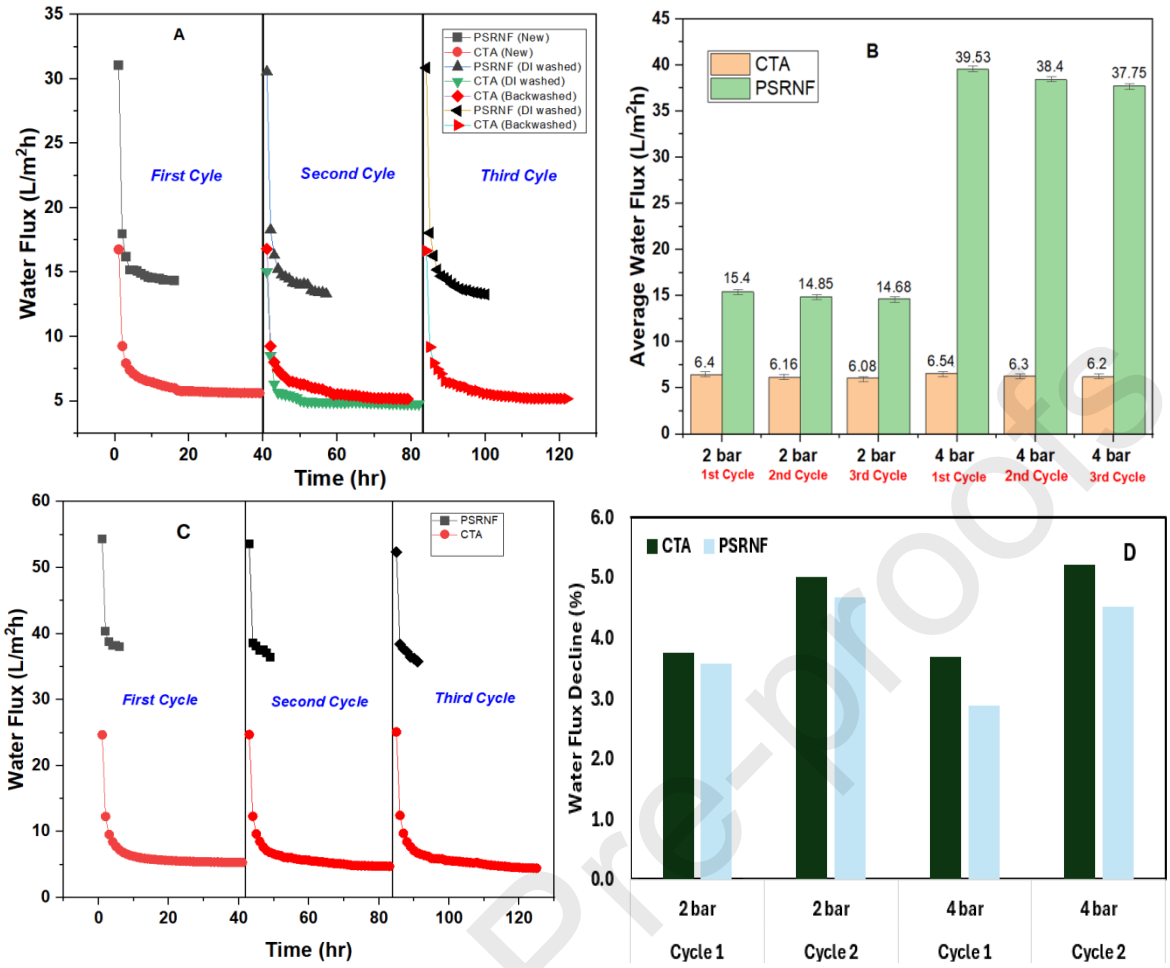

Figure 4. A) Water flux for the CTA and PSRNF membranes at 2 bar pressure for three cycles (cycle one represents the pristine membranes, cycle two represents the first wash for the PSRNF membrane with DI water at 40 °C, and first backwash for the CTA membrane, cycle three represents the second wash for the PSRNF membrane with DI water at 40 °C, and second backwash for the CTA membrane, B)Average permeation flux both membrane at 2 and 4 bar pressure for three cycles, C) Water flux for the CTA and PSRNF membranes at 4 bar pressure for three cycles, and D) Water flux decline in the CTA and PSRNF.

3.4 Membrane autopsy

The pristine and washed CTA and PSRNF membranes were examined and compared by FT-IR (Thermo Scientific Nicolet spectrometer), SEM (Scanning Electronic Microscope), and EDX (Bruker SDD X flash 5030). A comparison of FT-IR spectra between the pristine, DI-washed, and backwashed CTA membrane **(Figure 5A)** shows a significant peak at (~3550-3850 cm^{-1}) for the DI-washed CTA membrane where the O-H stretching variations resulting from the residual hydroxyl group of foulants on the membrane which resulted in the 16% water flux declining. The 2800-3000 cm^{-1} peaks correspond to C-H stretching vibrations from aliphatic hydrocarbon chains in the cellulose backbone. The firm peaks in the triacetate structure are caused by C-H bonds in the methyl (CH_3) and methylene (CH_2) groups. The peaks at ~2920 cm^{-1} in the spectra represent asymmetric and symmetric C-H bond stretching, respectively [38]. The used membranes' characteristic peaks appear at ~1735 cm^{-1}, indicating

the ester group's C=O (carbonyl) stretching as a result of the alkalinity of the wastewater. Ester connections cause a prominent peak at ~1235 cm^{-1} due to C-O-C stretching. C-O stretching of the saccharide structure in the cellulose backbone is linked to peaks of about 1050 cm^{-1}. **(Figure 5B)** shows essential information about the PSRNF membrane functional groups; the Sulfonic Acid Group (S=O) peak at 1250 cm^{-1} represents the surface charge of the membrane that plays a significant role in the electrostatic repulsion between the membrane and PFOA. The peak at 1500 cm-1 displays a distinctive pattern that helps identify specific molecular structures, which is especially important for examining the polymer backbone and cross-linking within the membrane. There were no changes in the peak for the first and second wash compared to the pristine membrane, which indicated that the membrane did not alter its characteristics when exposed to alkaline wastewater. The C=O stretching, a prominent characteristic of carbonyl groups in many chemical compounds, exhibits strong absorption in the 1550–1650 cm^{-1} range. The precise location and shape of these peaks provide insights into the level of hydrogen bonding and cross-linking within the membrane, which play a crucial role in determining its selective permeability and overall effectiveness in filtration applications. Variations in peak intensities and shapes can signal surface functionalization or membrane degradation. The N–H stretching, showed by a peak in 2920 cm^{-1}, indicates hydrogen bonding and is commonly linked to amides in polyamide membranes. Similarly, broad absorption bands near the 3600-3750 cm^{-1} typically point to hydroxyl groups, indicating the presence of water or hydrogen-bonding interactions.

The SEM images of the pristine, DI-washed, and backwashed CTA membranes clearly show residual fouling materials on the DI-washed membrane, while the backwashed membrane appears almost free of fouling **(Figure 6A, 6B, 6C)**. These observations are also supported by the EDX spectrum **(Figure 7A, 7B, 7C)**, where visible signs of fouling, such as Ca, Cl, S, K, Na, and Ca, were detected on the surface of CTA washed with DI water, indicating possible calcium sulphate scale fouling. Backwashed CTA membrane analysis showed no signs of S and Ca on the surface, emphasizing its effectiveness in mitigating scale fouling after wastewater treatment. Similarly, the SEM images **(Figure 8A & 8B)** show no signs of fouling materials on the pristine and DI-washed PSRNF membranes, which is further confirmed by the EDX results **(Figure 9A, 9B)**. Compared to the CTA FO membrane, the lower fouling tendency of the PSRNF membrane is due to its higher hydrophilicity (**Table 1**) and smoother membrane surface **(Figures 6A and 8A)**. Accordingly, the PSRNF membrane requires lower maintenance than the commercial CTA membrane used in the FO process.

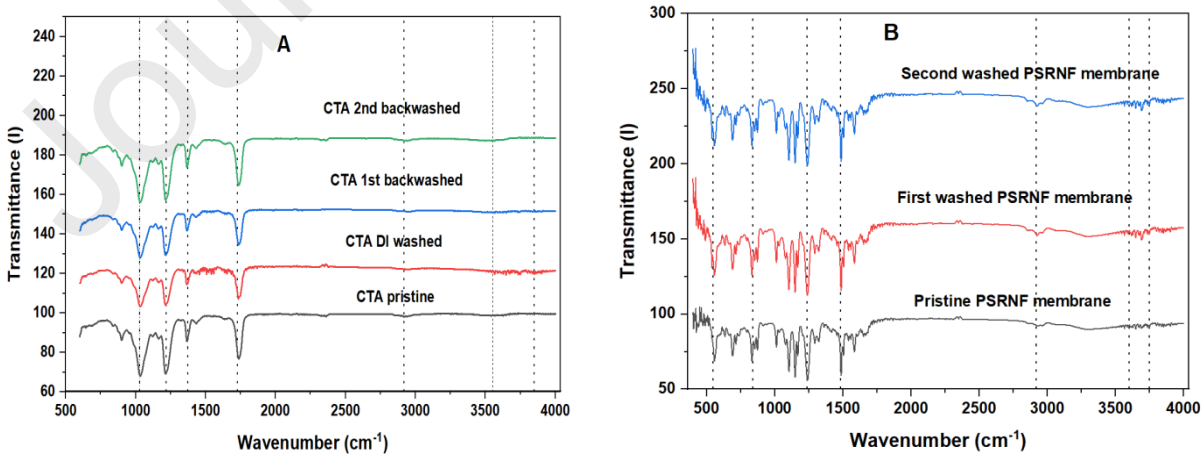

Figure 5. A) FT-IR spectra for the pristine, DI-washed, and backwashed CTA membrane, B) FT-IR spectra for the pristine and DI-washed PSRNF membrane.

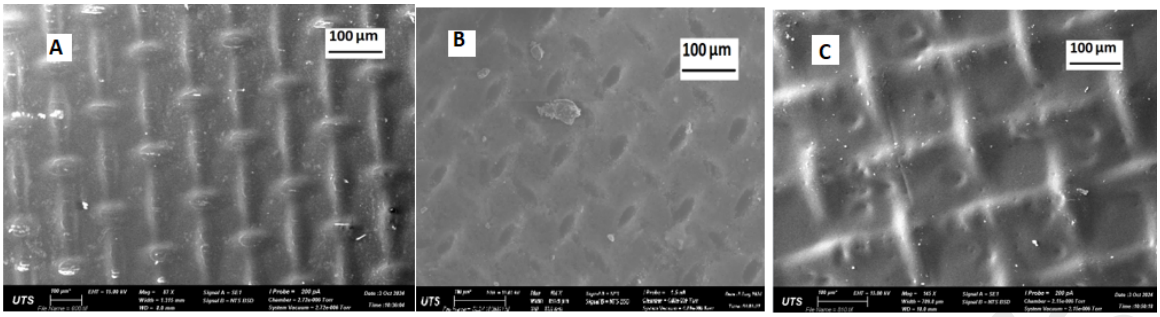

Figure 6. A) SEM image for the pristine CTA membrane, B) SEM image for the CTA membrane washed with DI water, and C) SEM image for the backwashed CTA membrane.

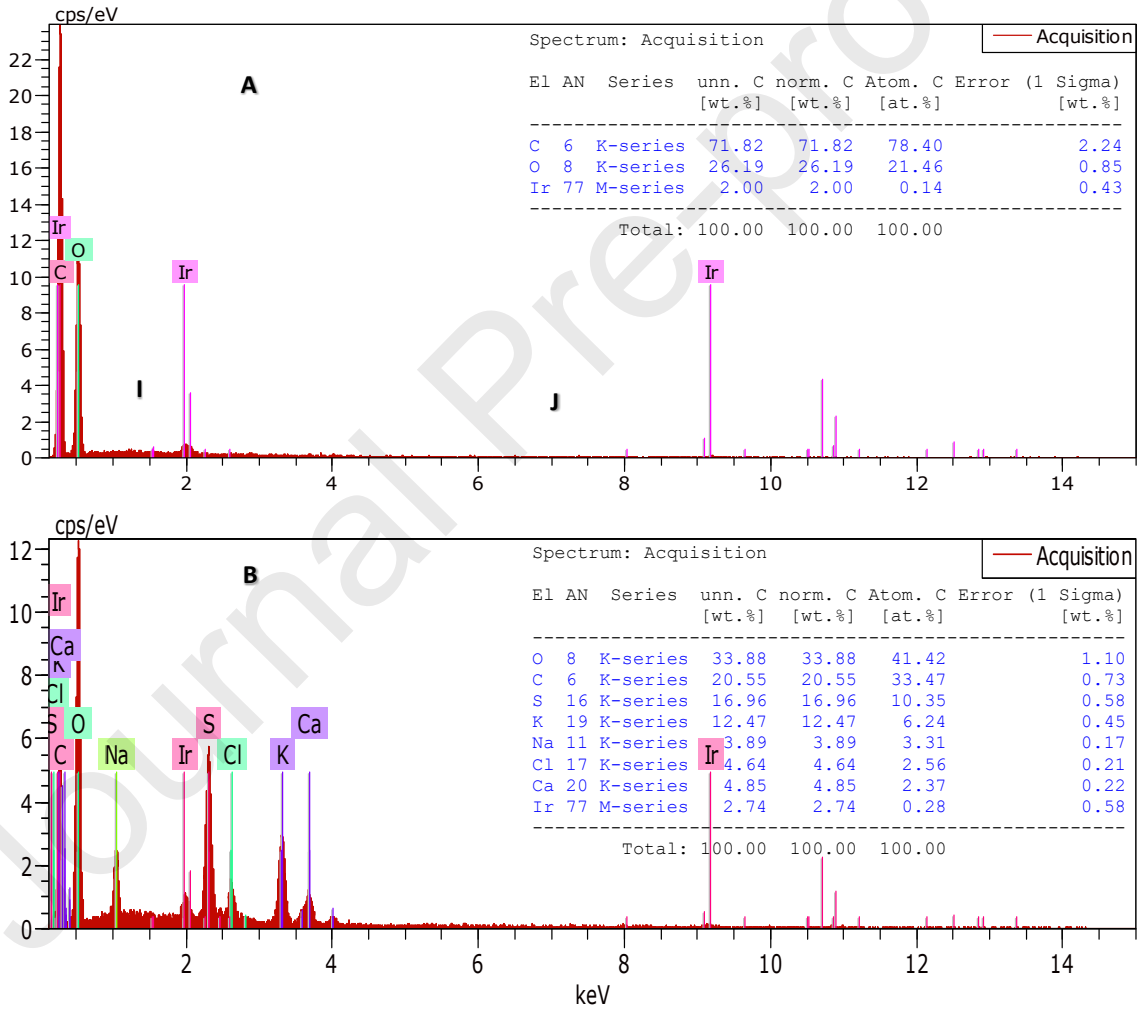

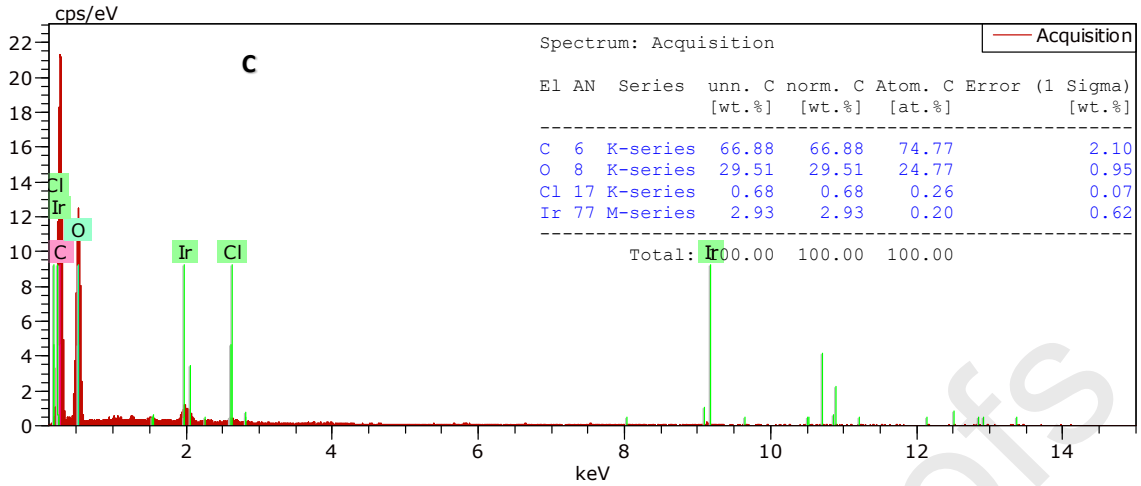

Figure 7. A) EDX analysis for the pristine CTA membrane, B) EDX analysis for the DI washed CTA membrane, C) EDX analysis for the backwashed CTA membrane.

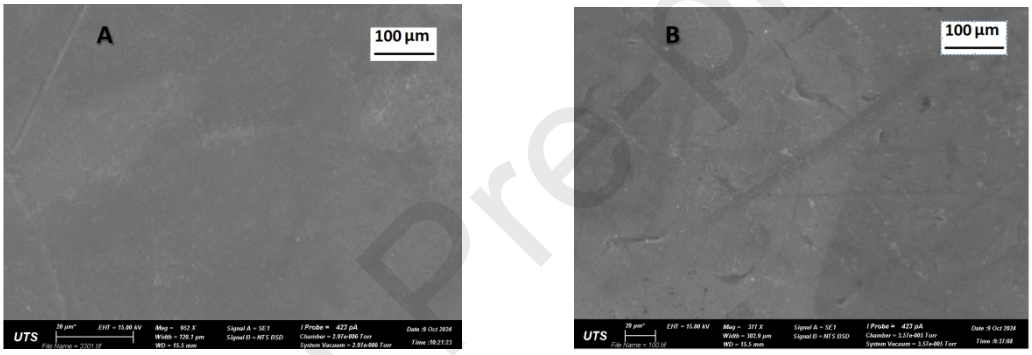

Figure 8. A) SEM image for the pristine PSRNF membrane, B) SEM image for the DI-washed PSRNF membrane.

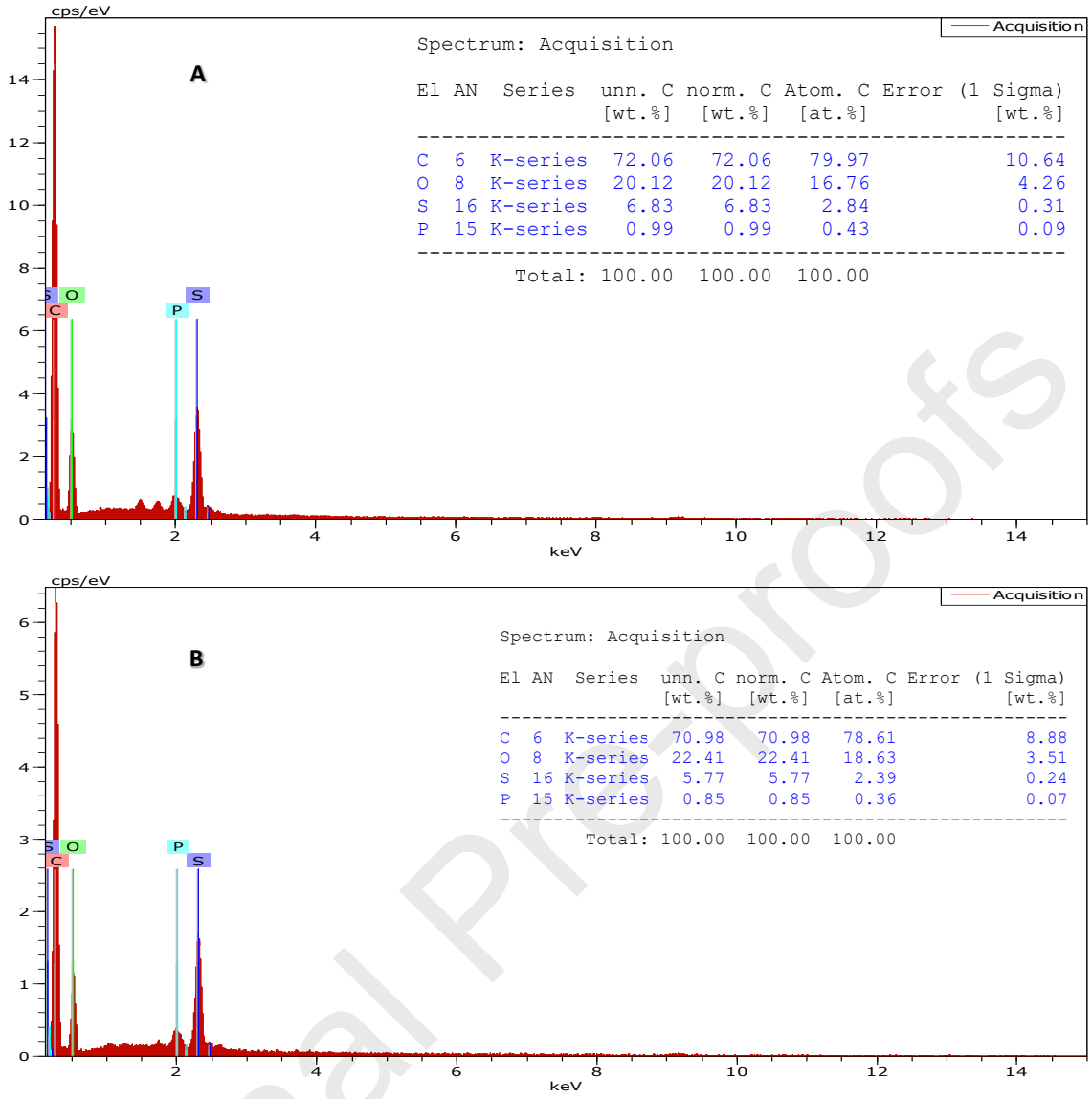

Figure 9. A) EDX analysis for the pristine PSRNF membrane, B) EDX analysis for the DI-washed PSRNF membrane.

3.5 Energy consumption and implications

The PSRNF membrane operates in the FO process within a range of 2 to 4 bar hydraulic pressure and 75% to 90% recovery rates, ensuring its competitivity with pressure-driven membrane processes. Energy consumption at 2 and 4 bar for both CTA and PSRNF membrane was calculated using Equation (8) based on 75% and 90% recovery rates, and the results are presented in **(Figure 6)**. At 2 bar feed pressure, the specific energy consumption of the PSRNF membrane for both 75% and 90% recovery rates were 0.016 kWh/m^3 and 0.018 kWh/m^3, respectively, compared to the CTA membrane of 0.04 kWh/m^3 and 0.048 kWh/m^3. The lower permeation flux and longer operation duration to achieve the 75% and 90% recoveries in the CTA experiments were the main reasons for its higher energy consumption compared to the PSRNF experiments.

At 75% recovery and 4 bar tests, the PSRNF membrane outperformed the CTA membrane by 86% less energy consumption **(Figure 6)** due to its higher permeation flux, resulting in a lower energy consumption according to Equation 8. Similarly, the energy consumption for the PSRNF membrane at 4 bar with a 90% recovery rate was only 0.011 kWh/m^3, which was almost 86% less than the specific energy consumption by the FO membrane at a similar operation parameter that recorded 0.083 kWh/m^3. Overall, the specific energy consumption was marginally higher in the tests with PSRNF and CTA membranes conducted at a 90% recovery rate due to the longer processing time. In comparison to the PSRNF membrane, the energy consumption for PFAS treatment by pressure-driven membrane processes was between 0.18 and 2.8 kWh/m^3 for the NF membranes [39, 40] and between 0.04 and 0.1 kWh/m^3 for the low-pressure RO membranes [32, 39].

The experimental results showed that the PSRNF TS80 membrane consumed the least energy without compromising its PFOA rejection efficiency. Therefore, using PSRNF membranes in the FO process offers an effective solution for treating wastewater by reducing the feed volume to 10% of its original volume and subsequently lowering treatment costs. Moreover, the commercially available PSRNF membrane is about tenfold cheaper than the commercially available CTA membrane. Its lower price, combined with a greater permeation flux achieved by applying just 4 bar feed pressure and a faster recovery rate, makes the PARNF membrane a promising candidate for treating PFOA-contaminated wastewater. This study used 0.6M NaCl and seawater as draw solutions for PFOA treatment in the CTA and PSRNF TS80 membranes, yet results showed superior performance for the PSRNF TS80 membrane at 2 and 4 bar over the commercial CTA membrane. The greater water flux in the PSRNF TS80 caused a greater dilution of the draw solution, but the water flux remained high due to its higher water permeability compared to the CTA membrane (**Table 1**). Further, the osmotic pressure of moderately concentrated brines, such as 0.6M NaCl and seawater, is enough for PFAS treatment by the FO process since PFAS contamination is of concern in terrestrial water resources, such as groundwater, lakes, and rivers of low TDS and osmotic pressure. In contrast, using a highly concentrated draw solution in the FO process causes a sharp drop in the water flux and increased reverse salt flux [19], let alone the cost of regenerating the draw solution.

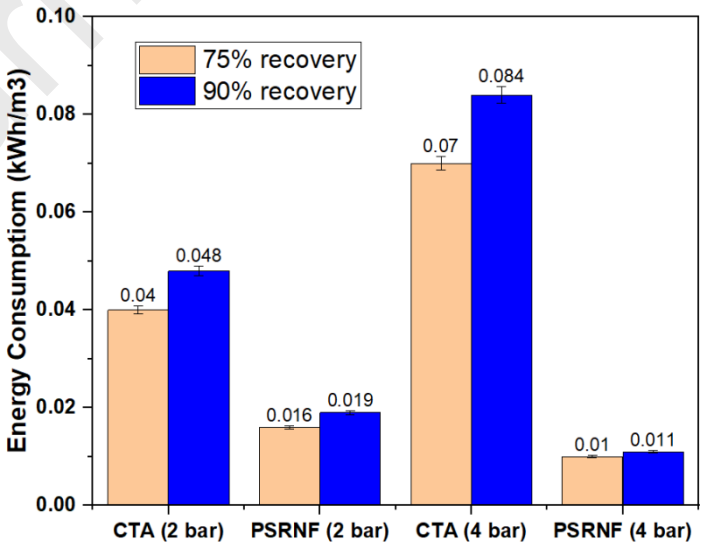

Figure 6. Energy consumption for the CTA and PSRNF membranes at 2 and 4 bar applied pressure for recovery rates of 75% and 90%.

4. Conclusion

This study demonstrated the promising potential of the PSRNF TS80 membrane in treating PFOA-contaminated wastewater. The membrane showed superior advantages compared to the CTA membranes for multiple critical metrics. Achieving up to 99.1 % PFOA rejection efficiency and six times higher average permeation flux up to 39.53 L/m²h at 4 bar compared to just 6.54 L/m²h for the CTA membrane under identical conditions. This performance is due to its enhanced hydrophilicity and water permeability coefficient. Besides the superior permeation flux efficiency of the PSRNF membrane, it achieved a 90% recovery rate in 6 hours at 4 bar, compared to 41 hours for the CTA membrane to reach the same recovery rate. Moreover, the PSRNF membrane energy consumption was recorded as low as 0.011 kWh/m³ at 4 bar for the 90% recovery rate, about 86.74% less energy consumption compared to the CTA membrane that consumed 0.083 kWh/m³ under similar conditions.

The PSRNF membrane showed tolerance to different FS conditions, such as pH, ionic strength, and PFOA concentrations. In comparison to the CTA membrane, the PSRNF TS80 membrane offered comparable or even better PFOA rejection efficiency as the applied pressure of the feed side increased from 0 to 4 bar and considerably higher water flux. Moreover, the PSRNF membrane's tolerance to alkaline feed and minimally impacted by fouling, with flux recovery exceeding 95% after simple cleaning with hot DI water at 40°C), with an effective reuse across multiple cycles while the necessity of more sophisticated osmotic backwash for the CTA membrane. The findings of this investigation suggest that the PSRNF TS80 membrane could have a greater impact on PFOA-contaminated wastewater treatment technology for its energy efficiency and fouling resistance, which subsequently increases the plant's lifetime and reduces costs. The superiority of the PSRNF membrane could be investigated for treating a wider range of PFAS, especially short-chain species. It would be beneficial to include a future outlook section regarding the scalability of PSRNF membranes in large-scale wastewater treatment plants.

References

1. Anderson, R.H., et al., *US Department of Defense–funded fate and transport research on per-and polyfluoroalkyl substances at aqueous film–forming foam–impacted sites.* Environmental Toxicology and Chemistry, 2021. **40**(1): p. 37.

2. Abunada, Z., M.Y. Alazaiza, and M.J. Bashir, *An overview of per-and polyfluoroalkyl substances (PFAS) in the environment: Source, fate, risk and regulations.* Water, 2020. **12**(12): p. 3590.

3. Deepika, D., et al., *Risk assessment of perfluorooctane sulfonate (PFOS) using dynamic age dependent physiologically based pharmacokinetic model (PBPK) across human lifetime.* Environmental Research, 2021. **199**: p. 111287.

4. Buck, R.C., et al., *Perfluoroalkyl and polyfluoroalkyl substances in the environment: terminology, classification, and origins.* Integrated environmental assessment and management, 2011. **7**(4): p. 513-541.

5. Thompson, J., et al., *Use of simple pharmacokinetic modeling to characterize exposure of Australians to perfluorooctanoic acid and perfluorooctane sulfonic acid.* Environment international, 2010. **36**(4): p. 390-397.

6. Calafat, A.M., et al., *Serum concentrations of 11 polyfluoroalkyl compounds in the US population: data from the National Health and Nutrition Examination Survey (NHANES) 1999− 2000.* Environmental science & technology, 2007. **41**(7): p. 2237-2242.

7. Garg, S., et al., *Remediation of water from per-/poly-fluoroalkyl substances (PFAS) – Challenges and perspectives.* Journal of Environmental Chemical Engineering, 2021. **9**(4): p. 105784.

8. Sun, M., et al., *Legacy and Emerging Perfluoroalkyl Substances Are Important Drinking Water Contaminants in the Cape Fear River Watershed of North Carolina.* Environmental Science & Technology Letters, 2016. **3**(12): p. 415-419.

9. de Vera, G.A. and E.C. Wert, *Using discrete and online ATP measurements to evaluate regrowth potential following ozonation and (non) biological drinking water treatment.* Water research, 2019. **154**: p. 377-386.

10. Baudequin, C., et al., *Removal of fluorinated surfactants by reverse osmosis–role of surfactants in membrane fouling.* Journal of membrane science, 2014. **458**: p. 111-119.

11. Tang, C.Y., et al., *Use of reverse osmosis membranes to remove perfluorooctane sulfonate (PFOS) from semiconductor wastewater.* Environmental science & technology, 2006. **40**(23): p. 7343-7349.

12. Ahmed, M.B., et al., *Advanced treatment technologies efficacies and mechanism of per-and poly-fluoroalkyl substances removal from water.* Process Safety and Environmental Protection, 2020. **136**: p. 1-14.

13. Zhi, Y., et al., *Removing emerging perfluoroalkyl ether acids and fluorotelomer sulfonates from water by nanofiltration membranes: Insights into performance and underlying mechanisms.* Separation and Purification Technology, 2022. **298**: p. 121648.

14. Hang, X., et al., *Removal and recovery of perfluorooctanoate from wastewater by nanofiltration.* Separation and Purification Technology, 2015. **145**: p. 120-129.

15. Wang, T., et al., *Fabrication of novel poly(m-phenylene isophthalamide) hollow fiber nanofiltration membrane for effective removal of trace amount perfluorooctane sulfonate from water.* Journal of Membrane Science, 2015. **477**: p. 74-85.

16. Zhao, C., et al., *Perfluorooctane sulfonate removal by nanofiltration membrane the role of calcium ions.* Chemical Engineering Journal, 2013. **233**: p. 224-232.

17. Ibrar, I., et al., *Challenges and potentials of forward osmosis process in the treatment of wastewater.* Critical Reviews in Environmental Science and Technology, 2020. **50**(13): p. 1339-1383.

18. Yan, M., et al., *High-performance thin film composite forward osmosis membrane for efficient rejection of antimony and phenol from wastewater: Characterization, performance, and MD-DFT simulation.* Journal of Membrane Science, 2024. **703**: p. 122847.

19. Aedan, Y., et al., *Perfluorooctanoic acid-contaminated wastewater treatment by forward osmosis: Performance analysis.* Science of The Total Environment, 2024: p. 173368.

20. Lee, C.-m., et al., *Performance analysis of serially-connected membrane element for pressure-assisted forward osmosis: Wastewater reuse and seawater desalination.* Desalin Water Treat, 2020. **183**: p. 104-113.

21. Khanafer, D., et al., *Performance of the Pressure Assisted Forward Osmosis-MSF Hybrid Desalination Plant.* Water, 2021. **13**(9): p. 1245.

22. Coday, B.D., et al., *Effects of transmembrane hydraulic pressure on performance of forward osmosis membranes.* Environmental science & technology, 2013. **47**(5): p. 2386-2393.

23. Khanafer, D., et al., *Innovative stimuli-responsive membrane MSF brine rejection dilution by tertiary treated sewage effluent.* Journal of Environmental Management, 2024. **365**: p. 121517.

24. Jamil, S., S. Jeong, and S. Vigneswaran, *Application of pressure assisted forward osmosis for water purification and reuse of reverse osmosis concentrate from a water reclamation plant.* Separation and Purification Technology, 2016. **171**: p. 182-190.

25. Wu, Z., et al., *Forward osmosis promoted in-situ formation of struvite with simultaneous water recovery from digested swine wastewater.* Chemical Engineering Journal, 2018. **342**: p. 274-280.

26. Xie, M., et al., *Comparison of the removal of hydrophobic trace organic contaminants by forward osmosis and reverse osmosis.* Water research, 2012. **46**(8): p. 2683-2692.

27. Madsen, H.T., et al., *Pressure retarded osmosis from hypersaline solutions: Investigating commercial FO membranes at high pressures.* Desalination, 2017. **420**: p. 183-190.

28. Zhang, S., et al., *Sustainable water recovery from oily wastewater via forward osmosis-membrane distillation (FO-MD).* water research, 2014. **52**: p. 112-121.

29. Altaee, A., D. Khanafer, and A. Hawari, *METHOD, APPARATUS AND SYSTEM FOR SEAWATER TREATMENT*. 2024.

30. Twohig, M., et al., *Approaches to Non-targeted Analyses of Per-and Polyfluoroalkyl Substances (PFAS) in Environmental Samples.* Waters Corp Application Note 720007184en, 2021.

31. Archer, A.C., A.M. Mendes, and R.A. Boaventura, *Separation of an anionic surfactant by nanofiltration.* Environmental science & technology, 1999. **33**(16): p. 2758-2764.

32. Xiong, J., et al., *The rejection of perfluoroalkyl substances by nanofiltration and reverse osmosis: influencing factors and combination processes.* Environmental Science: Water Research & Technology, 2021. **7**(11): p. 1928-1943.

33. Ibrar, I., et al., *Treatment of biologically treated landfill leachate with forward osmosis: Investigating membrane performance and cleaning protocols.* Science of The Total Environment, 2020. **744**: p. 140901.

34. Luo, Q., et al., *Preparation, characterization and performance of poly (m-phenylene isophthalamide)/organically modified montmorillonite nanocomposite membranes in removal of perfluorooctane sulfonate.* Journal of Environmental Sciences, 2016. **46**: p. 126-133.

35. Zazouli, M.A., et al., *Influences of solution chemistry and polymeric natural organic matter on the removal of aquatic pharmaceutical residuals by nanofiltration.* water research, 2009. **43**(13): p. 3270-3280.

36. Yu, Y., S. Lee, and S.K. Maeng, *Forward osmosis membrane fouling and cleaning for wastewater reuse.* Journal of Water Reuse and Desalination, 2017. **7**(2): p. 111-120.

37. Luo, J. and Y. Wan, *Effects of pH and salt on nanofiltration—a critical review.* Journal of membrane Science, 2013. **438**: p. 18-28.

38. Liu, C., et al., *Evaluating the efficiency of nanofiltration and reverse osmosis membrane processes for the removal of per-and polyfluoroalkyl substances from water: A critical review.* Separation and Purification Technology, 2022. **302**: p. 122161.

39. Jia, Z., et al., *Effects of cation exchange membrane properties on the separation of salt from high-salt organic wastewater by electrodialysis.* Chemical Engineering Journal, 2023. **475**: p. 146287.

40. Liu, C.J., et al., *Pilot-scale field demonstration of a hybrid nanofiltration and UV-sulfite treatment train for groundwater contaminated by per-and polyfluoroalkyl substances (PFASs).* Water research, 2021. **205**: p. 117677.